Coulomb wave functions in the theory of the circular paraboloidal waveguide

J. LoVetri[1]
Communications Security Establishment, Department of National Defence, P.O. Box 9703, Terminal, Ottawa, Ont., Canada K1G 3Z4
AND
M. Hamid[2]
Antenna Laboratory, Department of Electrical Engineering, University of Manitoba, Winnipeg, Man., Canada R2T 2N2
Received December 11, 1986[3]

In this paper it is shown how the Coulomb wave functions, commonly used in the description of a Coulomb field surrounding a nucleus, can be used in the description of electromagnetic fields that are symmetric with respect of ϕ inside a paraboloidal waveguide. The Abraham potentials Q and U, which are useful in describing fields with rational symmetry, are used to simplify the problem. It is shown that these potentials must satisfy a partial differential equation that when separated yields the Coulomb wave equation of order $L = 0$. Electromagnetic fields due to simple source distributions inside the paraboloid are expanded in terms of these functions. Specifically, solutions for current-loop sources located in the focal plane of the paraboloid are obtained. The case where the wall of the paraboloidal waveguide is assumed to be perfectly conducting is treated as well as the case where the wall has finite impedance. The finite paraboloid is also considered, and the far field is formulated using Huygen's principle. It is found that for the finite surface-impedance case, the far-field pattern due to a current loop operating at 100 MHz in the focal plane of a paraboloidal reflector of 1 m focal length is different from the perfectly conducting case. Specifically, the pattern seems to be more omnidirectional for the impedance case than for the perfectly conducting case. Numerical results are presented for relevant aspects of the problem.

Dans cet article, on montre comment les fonctions d'onde de Coulomb, communément utilisées dans la description d'un champ de Coulomb autour d'un noyau, peuvent être utilisées dans la description de champs électromagnétiques qui sont symétriques par rapport à ϕ à l'intérieur d'un guide d'onde paraboloïdal. Les potentiels Q et U d'Abraham, qui sont utiles pour la description de champs ayant une symétrie de rotation, sont utilisés afin de simplifier le problème. On montre que ces potentiels doivent satisfaire à une équation aux dérivées partielles qui donne, après séparation des variables, l'équation d'onde de Coulomb d'ordre $L = 0$. Les champs électromagnétiques dus à des distributions simples de sources à l'intérieur du paraboloïde sont développés en séries de ces fonctions. Spécifiquement, on obtient des solutions pour des sources en forme d'anneaux de courants placés dans le plan focal du paraboloïde. On traite le cas où la paroi du guide d'onde paraboloïdal est supposée parfaitement conductrice aussi bien que le cas où le paroi a une impédance finie. On considère aussi le paraboloïde fini, et le champ lointain est déterminé en utilisant le principe de Huygens. On montre que dans le cas d'une surface d'impédance finie, la configuration du champ lointain dû à un anneau de courant à 100 MHz placé dans le plan focal d'un réflecteur paraboloïdal de 1 m de distance focale est différente de celle qu'on obtient dans le cas d'une surface parfaitement conductrice. On présente des résultats numériques pour les aspects pertinents du problème.

[Traduit par la revue]

Can. J. Phys. **66**, 212 (1988)

1. Introduction

Perhaps the most common type of communications antenna is the circular parabolic type, which has a surface generated by revolving a finite parabolic curve about its axis. The reflector is then usually illuminated by an electromagnetic source positioned at or near the focal point. The reason for using the circular paraboloidal reflector is that from the theory of geometrical optics or ray optics, the circular paraboloidal shape has the property that all rays originating from the focus are reflected from the surface parallel to the axis. Most electromagnetic solutions of the paraboloidal reflector use the geometrical optics approximation. This is, in general, a high-frequency method and thus it is not an exact solution.

One of the classic methods of determining exact solutions in electromagnetic problems is to solve Maxwell's equations directly for the geometry, material, and sources under consideration. Solving Maxwell's equations can usually be reduced to finding the solutions of the vector wave equation or, for time-harmonic problems, the vector Helmholtz equation. It would probably be safe to say that most electromagnetic solutions are directly or indirectly related to the solution of the vector wave equation.

In terms of the orthogonal coordinate systems in which solutions can be obtained, the scalar Helmholtz equation can be solved using the method of separation of variables in 11 orthogonal coordinate systems. The rotation-paraboloidal coordinate system is one of the 11 orthogonal coordinate systems in which the scalar Helmholtz equation separates (see refs. 1–3). The situation is quite different with the vector wave equation or the vector Helmholtz equation (ref. 4). The complications arise because the field is a vector field and the vector equation cannot be separated into individual ordinary differential equations in which each scalar component exists decoupled from the remaining components. Also, even if this were possible, the fitting of the boundary conditions becomes almost impossible.

The first theoretical investigation of electromagnetic fields in rotation-paraboloidal coordinates was undertaken by Abraham (5). The paraboloidal coordinates were used to model a semi-infinite wire. The theoretical results did not agree with the experimental results available at the time and the problem was dropped. The electromagnetic reflection by a parabolic mirror was briefly mentioned by Lamb (6), where integral expressions were obtained. The problem was not reconsidered until the parabolic reflector was used for radar applications in the 1940s.

[1]Present address: Division of Electrical Engineering, National Research Council, Ottawa, Ont., Canada K1A 0R6.

[2]On leave at the Department of Electrical Engineering and Communication Sciences, University of Central Florida.

[3]Revision received August 6, 1987.

For the acoustic case, Buchholtz analyzed many aspects of the problem. He obtained reults in integral and series form for the scattering of acoustic waves from an infinite paraboloid (7). The external (convex side) diffraction problem has been analyzed by Horton and Karal (8, 9). Horton used the series representations developed by Pinney (10) for the solution of the scalar Helmholtz equation in rotation-paraboloidal coordinates. Pinney developed his series representation in terms of Laguerre functions, whereas Buchholtz used the confluent hypergeometric functions, which have a more general form.

The cases of an electric dipole at the focus of the paraboloid and oriented parallel to the axis of symmetry, perpendicular to the axis of symmetry, and perpendicular to the axis backed by a dummy reflector were solved by Pinney (11). The solutions to these three cases were based on the series solutions he obtained in his earlier paper for the scalar Helmholtz equation in rotation-paraboloidal coordinates. The exact electromagnetic field produced by an electric dipole located on the axis of symmetry of a perfectly conducting concave paraboloid has also been solved by Buchholtz (12). Fock (13) has performed an in-depth study of the problem, expressing the exact solution for an electric dipole at the focus and perpendicular to the axis of symmetry, both as an integral and as an infinite series, as well as deriving high-frequency expansions.

Fock first expresses Maxwell's equations in terms of the covariant spherical-field components and the Debye potentials (see ref. 14). From these he applies the transformation to obtain the rotation-paraboloidal field components. He then introduces two "parabolic potentials P and Q," which are connected with the separate Fourier components of the field with respect to the angle, ϕ, and not the total field. He simplifies the field expressions by introducing four interrelated auxiliary functions connected with the parabolic potentials P and Q. Although the introduction of the parabolic potentials permits formulation of the boundary conditions without recourse to finite-difference equations, the expressions are very complicated even for simple source illuminations.

The problem under consideration in Horton and Karal's work was the electromagnetic scattering of a plane wave from a paraboloid made of any material in general (15). The Hansen wave vectors were obtained for the rotation-paraboloidal coordinate system based on the series solution obtained by Pinney (10) for the scalar Helmholtz equation. This was done even though the transverse vectors $\boldsymbol{M}$ and $\boldsymbol{N}$ did not appear to have the necessary orthogonality properties to enable one to expand an arbitrary vector function in terms of them directly. Considerable manipulations were then performed to use the orthogonality properties of one of Pinney's paraboloidal functions S_ν^μ, which is related to the Laguerre functions. The final field expressions using this method are very complicated. Solutions for a plane wave incident upon a perfectly conducting paraboloid are formulated, but no numerical results are presented because of a "lack of numerical values for the paraboloidal functions."

Approximate methods have been used by Donaldson *et al.* (16) to solve for the aperture distribution due to axially oriented dipoles at the focal point. In this paper, the paraboloid of revolution is instead treated as a waveguide and fields, which are rotationally symmetric but arbitrary (i.e., the field components are independent of ϕ), are found in terms of the Abraham potentials (see refs. 2 or 17). Eigenfunctions are obtained for the paraboloid in terms of the Coulomb wave functions. This technique of treating the paraboloid as a waveguide allows one to apply an impedance boundary condition on the walls of the paraboloid. This is a technique that can be used for simulating mathematically the finite conductivity of the walls or can even be used when deliberate or nondeliberate thin coatings of dielectric are applied to the walls, e.g., absorbing materials and rain, etc. This problem is difficult to solve if geometrical optics is used, but in the present technique it means only the determination of the new eigenvalues. Thus for each new boundary condition that we wish to solve (i.e., different wall impedance), all we need to do is calculate the new eigenvalues. This is one of the main advantages of this method.

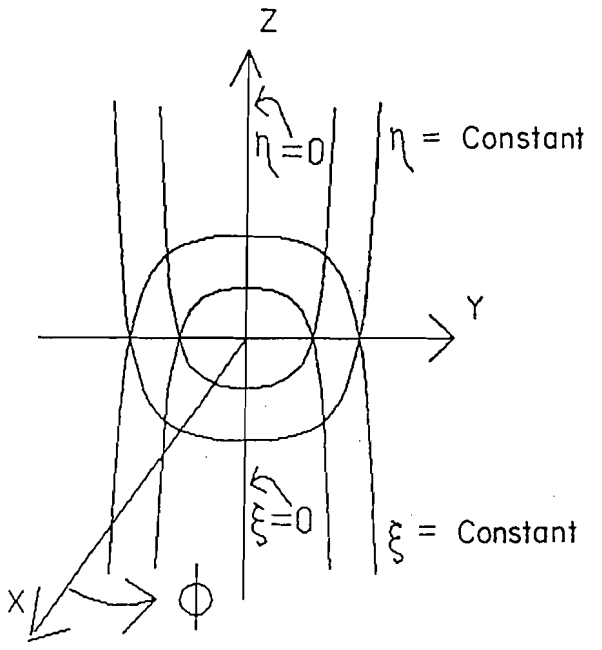

FIG. 1. Rotation-paraboloidal coordinates.

2. Formulation with Abraham potentials

The rotation-paraboloidal coordinate system (ξ, η, ϕ), see Fig. 1, is related to the rectangular coordinate system (x, y, z), the circular cylindrical coordinate system (ρ, ϕ, z), and the spherical coordinate system (r, θ, ϕ) by the transformations

[1] $x = \xi\eta\cos\phi = \rho\cos\phi = r\sin\theta\cos\phi$

[2] $y = \xi\eta\sin\phi = \rho\sin\phi = r\sin\theta\sin\phi$

[3] $z = \frac{1}{2}(\xi^2 - \eta^2) = z = r\cos\theta$

The scale factors can be obtained from [1]–[3]

[4] $h_1 = h_2 = \sqrt{\xi^2 + \eta^2} = 2r$

and

[5] $h_3 = \xi\eta = \rho$

where, of course, $\rho^2 = x^2 + y^2$ and $r^2 = x^2 + y^2 + z^2$.

If a harmonic time dependence of $e^{-i\omega t}$ is assumed, then Maxwell's equations can be written as

[6] $\nabla \times \boldsymbol{E} = i\omega\mu\boldsymbol{H}$

[7] $\nabla \times \boldsymbol{H} = (-i\omega\epsilon + \sigma)\boldsymbol{E}$

[8] $\nabla \times \boldsymbol{H} = -i\omega\epsilon\boldsymbol{E}$, lossless medium

[9] $\nabla \cdot \boldsymbol{H} = 0$

[10] $\nabla \cdot \boldsymbol{E} = \frac{\rho_c}{\epsilon}$

In the above, ρ_c is the charge density in the medium, ϵ is the permittivity of the medium, μ is the permeability of the medium, and ω is the harmonic frequency of the excitation. These must now be expressed in terms of the rotation-paraboloidal coordinate system.

For the case where the field ($\boldsymbol{E}$ and $\boldsymbol{H}$) itself has the same symmetry as the coordinate system, its components are independent of ϕ. Thus, Maxwell's equations break up into the two independent groups:

$$[11]\quad \frac{1}{\xi^2+\eta^2}\left[\frac{\partial}{\partial\xi}(\sqrt{\xi^2+\eta^2}\,H_\eta)-\frac{\partial}{\partial\eta}(\sqrt{\xi^2+\eta^2}\,H_\xi)\right] + i\omega\epsilon E_\phi = 0$$

$$[12]\quad \frac{1}{\rho\sqrt{\xi^2+\eta^2}}\frac{\partial}{\partial\eta}(\rho E_\phi) - i\omega\mu H_\xi = 0$$

$$[13]\quad \frac{1}{\rho\sqrt{\xi^2+\eta^2}}\frac{\partial}{\partial\xi}(\rho E_\phi) + i\omega\mu H_\eta = 0$$

$$[14]\quad \frac{1}{\xi^2+\eta^2}\left[\frac{\partial}{\partial\xi}(\sqrt{\xi^2+\eta^2}\,E_\eta)-\frac{\partial}{\partial\eta}(\sqrt{\xi^2+\eta^2}\,E_\xi)\right] - i\omega\mu H_\phi = 0$$

and

$$[15]\quad \frac{1}{\rho\sqrt{\xi^2+\eta^2}}\frac{\partial}{\partial\eta}(\rho H_\phi) + i\omega\epsilon E_\xi = 0$$

$$[16]\quad \frac{1}{\rho\sqrt{\xi^2+\eta^2}}\frac{\partial}{\partial\xi}(\rho H_\phi) - i\omega\epsilon E_\eta = 0$$

where $\rho = \xi\eta$. Substituting [12] and [13] into [11], and defining the Abraham potential $U(\xi, \eta)$ as

$$[17]\quad E_\phi(\xi,\eta) = \frac{1}{\rho}U(\xi,\eta)$$

we find that

$$[18]\quad H_\xi(\xi,\eta) = \frac{-i\omega\epsilon}{\rho K^2\sqrt{\xi^2+\eta^2}}\frac{\partial U(\xi,\eta)}{\partial\eta}$$

$$[19]\quad H_\eta(\xi,\eta) = \frac{i\omega\epsilon}{\rho K^2\sqrt{\xi^2+\eta^2}}\frac{\partial U(\xi,\eta)}{\partial\xi}$$

where $U(\xi, \eta)$ satisfies

$$[20]\quad \frac{\partial}{\partial\xi}\left(\frac{1}{\rho}\frac{\partial U}{\partial\xi}\right)+\frac{\partial}{\partial\eta}\left(\frac{1}{\rho}\frac{\partial U}{\partial\eta}\right)+\frac{K^2}{\rho}(\xi^2+\eta^2)U = 0$$

Similarly, if the same procedure is applied to [24], the second Abraham potential $Q(\xi, \eta)$ can be defined as

$$[21]\quad H_\phi(\xi,\eta) = \frac{1}{\rho}Q(\xi,\eta)$$

with

$$[22]\quad E_\xi(\xi,\eta) = \frac{i\omega\mu}{\rho K^2\sqrt{\xi^2+\eta^2}}\frac{\partial Q(\xi,\eta)}{\partial\eta}$$

$$[23]\quad E_\eta(\xi,\eta) = \frac{-i\omega\mu}{\rho K^2\sqrt{\xi^2+\eta^2}}\frac{\partial Q(\xi,\eta)}{\partial\xi}$$

where $Q(\xi, \eta)$ satisfies

$$[24]\quad \frac{\partial}{\partial\xi}\left(\frac{1}{\rho}\frac{\partial Q}{\partial\xi}\right)+\frac{\partial}{\partial\eta}\left(\frac{1}{\rho}\frac{\partial Q}{\partial\eta}\right)+\frac{K^2}{\rho}(\xi^2+\eta^2)Q = 0$$

The potential $U(\xi, \eta)$ represents an electromagnetic wave transverse electric to the z direction (i.e., TE to z), and the second potential $U(\xi, \eta)$ represents an electromagnetic wave transverse magnetic to the z direction (i.e., TM to z). However, both U and Q satisfy the same partial differential equation; that is, [20] and [24]. This suggests that the potentials U and Q should be similar but not exactly the same because the boundary conditions on the walls of the paraboloid are different for each potential. Moreover, a singularity in the field along the axis of the paraboloid seems possible owing to the forms of the expressions of [17] and [21] because $\rho = 0$ along this axis. Solutions to the potentials are chosen such that they are equal to zero at $\rho = 0$ and that in the limit as ρ goes to zero, the field expressions remain finite.

3. Boundary conditions for the potentials

If the surface of the parabaloid ($\eta = \eta_0$) is perfectly conducting, then a Neumann condition for the potential $Q(\xi, \eta)$ arises,

$$[25]\quad \frac{\partial Q(\xi,\eta)}{\partial\eta} = 0, \qquad \eta = \eta_0$$

and a Dirichlet condition for the potential $U(\xi, \eta)$ arises,

$$[26]\quad U(\xi,\eta_0) = 0$$

Thus for the perfectly conducting paraboloidal waveguide, the Abraham potentials $U(\xi, \eta)$ and $Q(\xi, \eta)$ must satisfy partial differential equations given by [20] and [24] respectively, with boundary conditions at $\eta = \eta_0$ described by [26] and [25], respectively.

For the nonperfectly conducting paraboloidal waveguide, an impedance or Leontovich boundary condition is imposed on the surface $\eta = \eta_0$. The Leontovich boundary condition can be expressed mathematically as

$$[27]\quad \boldsymbol{E} - (\boldsymbol{E}\cdot\hat{\boldsymbol{n}})\hat{\boldsymbol{n}} = \overleftrightarrow{N}\sqrt{\frac{\mu}{\epsilon}}(\hat{\boldsymbol{n}}\times\boldsymbol{H})$$

where $\overleftrightarrow{N}$ is the relative surface impedance of the walls of the paraboloid ($N = 0$ for the perfectly conducting case) and $\hat{n}$ is the unit normal to the surface. As can be seen, the relative surface impedance is represented as a dyadic function. A nonzero surface impedance has been used for the finite conductivity of waveguides before (see ref. 18). It has also been used to account for the finite conductivity of scatterers (19), for the roughness of its surface (20), and for the presence of highly absorbing coating layers (21).

If $\overleftrightarrow{N}$ had been assigned a scalar value, this would imply that the impedance is the same in any direction, but this is not the general case. In the more general case considered here, the surface impedance $\overleftrightarrow{N}$ is represented by a two-dimensional dyadic transforming the tangential components of $\boldsymbol{H}$ into the tangential components of $\boldsymbol{E}$ on the boundary (see ref. 3, p. 1814).

It is found that the Leontovich condition manifests itself in the two equations

$$[28]\quad \frac{E_\xi}{H_\phi} = -N_\xi\sqrt{\frac{\mu}{\epsilon}}, \qquad \eta = \eta_0$$

and

$$[29]\quad \frac{E_\phi}{H_\xi} = N_\phi\sqrt{\frac{\mu}{\epsilon}}, \qquad \eta = \eta_0$$

Substitution of [17], [18] and [21], [22] into [29] and [28], respectively, leads to boundary conditions in terms of the potentials given by

$$[30]\quad U' - \frac{i\sqrt{\xi^2+\eta^2}}{\eta N_\phi} U = 0, \qquad \eta = \eta_0$$

and

$$[31]\quad Q' - \frac{iN_\xi}{\eta}\sqrt{\xi^2+\eta^2}\, Q = 0, \qquad \eta = \eta_0$$

If we assume, for the sake of mathematical simplicity, that

$$[32]\quad N_\phi = -\frac{i}{\eta_0}\sqrt{\xi^2+\eta_0^2}$$

and

$$[33]\quad N_\xi = \frac{i\eta_0}{\sqrt{\xi^2+\eta_0^2}}$$

then the boundary conditions on the potentials simplify to

$$[34]\quad U' + U = 0, \qquad \eta = \eta_0$$

and

$$[35]\quad Q' + Q = 0, \qquad \eta = \eta_0$$

These can be recognized as Dirichlet–Neumann or Robin boundary conditions and can be handled fairly easily by partial-differential-equation theory.

3.1. Solution for the potentials

Solutions to the partial differential equation given by [20] or [24] must now be found. It is sufficient to solve only one of these equations.

The method of separation of variables is used to solve [20]. This results in a solution of the form

$$[36]\quad U(\xi,\eta) = U_1(\xi)U_2(\eta)$$

If a separation constant C is chosen, then separation of the equation produces the two ordinary differential equations

$$[37]\quad \frac{d^2}{d\xi^2}U_1(\xi) - \frac{1}{\xi}\frac{d}{d\xi}U_1(\xi) + (K^2\xi^2 - C)U_1(\xi) = 0$$

and

$$[38]\quad \frac{d^2}{d\eta^2}U_2(\eta) - \frac{1}{\eta}\frac{d}{d\eta}U_2(\eta) + (K^2\eta^2 + C)U_2(\eta) = 0$$

These equations are identical except for the sign of the parameter C, but because the only restriction on the parameter is that it be a real number, only one of the equations need be solved. We choose [38], the equation for the variable η, as this equation will provide us with the eigenfunctions needed in later sections.

It can be shown (22) with the use of variable transformations that [38] can be reduced to a form recognized as the Coulomb wave equation of order $L = 0$

$$[39]\quad \frac{d^2}{dz^2}y(z) + \left[1 - \frac{2\beta}{z} - \frac{L(L+1)}{z^2}\right]y(z) = 0$$

where for the present case

$$[40]\quad \beta = -\lambda = -\frac{C}{4K}$$

The Coulomb wave equation has a regular singularity at the point $z = \infty$. The general solution of [39] is

$$[41]\quad y(z) = C_L F_l(\beta, z) + C_2 G_l(\beta, z)$$

where C_1 and C_2 are constants, F_L is the regular Coulomb wave function, and G_L is the irregular Coulomb wave function. For the specific case of $L = 0$, the solution can be written as

$$[42]\quad y(z) = C_1 F_0(\beta, z) + C_2 G_0(\beta, z)$$

The reason for introducing the negative sign in front of λ, in [40], is that when [39] is defined as a Sturm–Liouville system, it will prove to be more convenient, because λ will be defined as the eigenvalue. The mathematical properties of Coulomb wave functions used in this paper can be found in refs. 22 and 23. Some of the mathematical properties have been included herein as Appendix A.

The solutions for the Abraham potentials $U(\xi,\eta)$ and $Q(\xi,\eta)$ can be constructed using these Coulomb wave functions. The eigenfunctions are represented by the regular Coulomb wave functions $F_0(-\lambda_n, \frac{1}{2}K\eta^2)$ with the eigenvalues λ_n appropriately chosen so that the boundary conditions at $\eta = \eta_0$ will be satisfied. These boundary conditions can be either Dirichlet, Neumann, or Robin boundary conditions, whichever are required, as explained previously. The irregular Coulomb wave functions are not used as eigenfunctions because not only are they not orthogonal, but from [17] and [21] they would produce a singularity in the field at $\eta = 0$ (i.e., the axis of the paraboloid). The regular wave functions do not produce such a singularity because they produce a zero-over-zero term and L'Hopital's rule can be used to take the limit as η goes to 0. This limit turns out to be finite and thus there is no singularity.

In the ξ coordinate, the functions that will be used are $F_0(\lambda, \frac{1}{2}K\xi^2)$ (i.e., wave functions of the third kind, see Appendix A) for regions including the $\xi = 0$ axis and $H_0^1(\lambda, \frac{1}{2}K\xi^2)$ for regions not including the $\xi = 0$ axis. The reason that H_0^1 is chosen is clear from [A29] and the $e^{-i\omega t}$ time dependence, because these functions would best describe outward-travelling waves. Thus, the potentials can be constructed as

$$[43]\quad U(\xi,\eta) = \begin{cases} \sum_n A_n F_0(\lambda_n, \frac{1}{2}K\xi^2)F_0(-\lambda_n, \frac{1}{2}K\eta^2), & 0<\eta<\eta_0, \quad \xi = 0 \text{ region} \\ \sum_n B_n H_0^1(\lambda_n, \frac{1}{2}K\xi^2)F_0(-\lambda_n, \frac{1}{2}K\eta^2), & 0<\eta<\eta_0, \quad \xi = \text{large region} \end{cases}$$

and

$$[44]\quad Q(\xi,\eta) = \begin{cases} \sum_n A_n F_0(\lambda_n, \frac{1}{2}K\xi^2)F_0(-\lambda_n, \frac{1}{2}K\eta^2), & 0<\eta<\eta_0, \quad \xi = 0 \text{ region} \\ \sum_n B_n H_0^1(\lambda_n, \frac{1}{2}K\xi^2)F_0(-\lambda_n, \frac{1}{2}K\eta^2), & 0<\eta<\eta_0, \quad \xi = \text{large region} \end{cases}$$

and

The summation over n in the above equations represents a summation over the ordered eigenvalues, where the eigenvalues

$\lambda_n = C_n/4K$ are obtained from the transcendental equation produced by applying the boundary conditions on the walls of the waveguide. Eigenvalues for all three types of boundary conditions are given in the next section.

4. Eigenvalues and eigenfunctions

The application of specific boundary conditions to the field at $\eta = \eta_0$ results in specific boundary conditions for the potential U and Q. These boundary conditions determine the appropriate eigenvalues for the problem under consideration. From the Sturm–Liouville system theory we know that there is a denumerable number of eigenvalues that can be ordered according to ascending value (see refs. 24 and 25). It is also known that all the eigenvalues are positive in value except for a finite number of them. The three boundary conditions are now considered. The first few eigenvalues are calculated for all three cases along with the normalization constants N. For the perfectly conducting paraboloidal waveguide, the Dirichlet condition arises for the potential $U(\xi, \eta)$ and the Neumann condition arises for the potential $Q(\xi, \eta)$. Recall that the potential U represents circularly symmetric TE modes and the potential Q represents circularly symmetric TM modes inside the paraboloidal waveguide.

The transcendental equation that arises from applying the Dirichlet condition to U is obtained by applying [26] to [43] and can be simply written as

$$[45] \quad F_0(-\lambda_n, \tfrac{1}{2}K\eta_0^2) = 0$$

Thus all values of λ_n that satisfy this equation are the eigenvalues. The regular Coulomb wave function can be plotted as a function of the parameter λ_n (see ref. 22). The three frequencies, 100, 250, and 500 MHz, are chosen with a constant coordinate η_0 of the paraboloid corresponding to a focal length of 1 m. The zero crossings, which are the eigenvalues, are then obtained by a numerical technique, and the first few eigenvalues are shown in Table 1 for the respective frequencies.

For the Neumann condition, the transcendental equation that arises can be obtained by applying [25] to [44] and can be written as

$$[46] \quad F_0'(-\lambda_n, \tfrac{1}{2}K\eta_0^2) = 0$$

This function can also be plotted as a function of the parameter λ_n (see ref. 22). The same frequencies and size of paraboloid are chosen as for the Dirichlet case. Some eigenvalues with the respective normalization constants are shown in Table 2.

For the case where the walls are nonperfectly conducting or absorbing, the Robin condition arises for both potentials if we assume the wall impedances to be given by [32] and [33]. The transcendental equation is derived by applying [34] or [35] to [43] or [44]. This transcendental equation can be written as

$$[47] \quad F_0'(-\lambda_n, \tfrac{1}{2}K\eta_0^2) + F_0(-\lambda_n, \tfrac{1}{2}K\eta_0^2) = 0$$

This function, here called the Robin function, has also been plotted as a function of the parameter λ_n (see ref. 22). The zero crossings represent the eigenvalues, and these are found along with the normalization constants for the same frequencies and size of paraboloid as for the previous two cases. The first few eigenvalues and normalization constants are tabulated in Table 3.

The eigenfunctions for the potentials $U(\xi, \eta)$ and $Q(\xi, \eta)$ are given by the regular Coulomb wave functions with the parameter equal to the negative of the eigenvalue, $-\lambda_n$. These eigenfunctions are then normalized by the normalization constant N. Eigenfunctions for the case where the frequency is equal to 100 MHz are plotted in Figs. 2–4 for all three boundary-condition cases as indicated. As can be seen from these plots, the eigenfunctions all go to zero at $\eta = 0$. This is the condition that allows these functions to be orthogonal. Not all the components of the actual fields necessarily go to zero at $\eta = 0$ or $\xi = 0$, but care must be exercised in the evaluation of the fields at these points. The fields derived from the potential $U(\xi, \eta)$ are expressed analytically at these critical points. The fields derived from the potential $Q(\xi, \eta)$ are not shown explicitly here but can be derived by a similar procedure.

Expressions for the TE-mode fields can be obtained by substituting [43] into [17]–[19]. Thus,

$$[48] \quad E_\phi = \begin{cases} \sum_n \dfrac{A_n}{\xi\eta} F_0(\lambda_n, \tfrac{1}{2}K\xi^2)F_0(-\lambda_n, \tfrac{1}{2}K\eta^2), & 0 < \eta < \eta_0, \quad \xi = 0 \text{ region} \\ \sum_n \dfrac{B_n}{\xi\eta} H_0^1(\lambda_n, \tfrac{1}{2}K\xi^2)F_0(-\lambda_n, \tfrac{1}{2}K\eta^2), & 0 < \eta < \eta_0, \quad \xi > 0 \text{ region} \end{cases}$$

$$[49] \quad H_\xi = \frac{-i\omega\epsilon}{\xi K\sqrt{\xi^2 + \eta^2}} \begin{cases} \sum_n A_n F_0(\lambda_n, \tfrac{1}{2}K\xi^2)F_0'(-\lambda_n, \tfrac{1}{2}K\eta^2), & 0 < \eta < \eta_0, \quad \xi = 0 \text{ region} \\ \sum_n B_n H_0^1(\lambda_n, \tfrac{1}{2}K\xi^2)F_0'(-\lambda_n, \tfrac{1}{2}K\eta^2), & 0 < \eta < \eta_0, \quad \xi = 0 \text{ region} \end{cases}$$

$$[50] \quad H_\eta = \frac{i\omega\epsilon}{\eta K\sqrt{\xi^2 + \eta^2}} \begin{cases} \sum_n A_n F_0'(\lambda_n, \tfrac{1}{2}K\xi^2)F_0(-\lambda_n, \tfrac{1}{2}K\eta^2), & 0 < \eta < \eta_0, \quad \xi = 0 \text{ region} \\ \sum_n B_n H_0'(\lambda_n, \tfrac{1}{2}K\xi^2)F_0(-\lambda_n, \tfrac{1}{2}K\eta^2), & 0 < \eta < \eta_0, \quad \xi = 0 \text{ region} \end{cases}$$

To evaluate these expressions on either the $\xi = 0$ or the $\eta = 0$ axis, we take the limit and use L'Hopital's rule throughout. As $\eta \to 0$, the fields become

$$[51] \quad EH_\phi = 0, \qquad \eta = 0$$

$$[52]\quad H_\xi = \frac{-i\omega\epsilon}{K\xi^2}\begin{cases}\sum_n A_n F_0(\lambda_n, \frac{1}{2}K\xi^2)C_0(-\lambda_n), & \eta = 0, \quad \xi = 0 \text{ region}\\ \sum_n B_n H_0^1(\lambda_n, \frac{1}{2}K\xi^2)C_0(-\lambda_n), & \eta = 0, \quad \xi > 0 \text{ region}\end{cases}$$

$$[53]\quad H_\eta = 0, \qquad \eta = 0$$

where C_0 is given by [A9]. As can be seen at $\eta = 0$, only the H_ξ component survives. This is consistent with expectations as the field must be symmetric in ϕ.

As $\xi \to 0$, the fields become

$$[54]\quad E_\phi = 0, \qquad \xi = 0$$

$$[55]\quad H_\xi = 0, \qquad \xi = 0$$

$$[56]\quad H_\eta = \frac{i\omega\epsilon}{K\eta^2}\sum_n A_n C_0(\lambda_n)F_0(-\lambda_n, \tfrac{1}{2}K\eta^2), \qquad 0 < \eta < \eta_0, \qquad \xi = 0$$

This time only the η component of the magnetic field survives, as expected.

5. Current-loop excitation

Consider the case of an electric current sheet expressed by the following equation:

$$[57]\quad \boldsymbol{J}(\xi, \eta) = J_\phi(\eta)\delta(\xi - \xi^*)\hat{a}_\phi$$

where $\delta(\xi - \xi^*)$ represents the impulse function and $J_\phi(\eta)$ represents the magnitude of the current sheet. The dependence on η of the magnitude $J_\phi(\eta)$ is not shown explicitly as it is arbitrary. To simulate a current ring, we set the η dependence equal to the impulse function as well.

It is obvious that this specific excitation of [57] will produce fields that are independent of the coordinate ϕ. Thus, the Abraham potentials are appropriate, and in fact, it will become apparent that only the potential U will be necessary as the fields will be transverse electric (TE to the z axis).

The potential U can be represented in terms of an infinite summation of eigenfunctions where the Coulomb wave functions of the third kind are used in region II (i.e., in the region where $\xi > \xi^*$). The reason for this is that outward-travelling waves are desired in region II and these are best represented by wave functions of the third kind, i.e.,

$$[58]\quad U(\xi, \eta) = \begin{cases}\sum_n A_n F_0\left(\frac{C_n}{4K}, \frac{1}{2}K\xi^2\right)F_0\left(\frac{-C_n}{4K}, \frac{1}{2}K\eta^2\right), & 0 < \xi < \xi^*, \quad 0 < \eta < \eta_0\\ \sum_n B_n H_0^1\left(\frac{C_n}{4K}, \frac{1}{2}K\xi^2\right)F_0\left(\frac{-C_n}{4K}, \frac{1}{2}K\eta^2\right), & \xi > \xi^*, \quad 0 < \eta < \eta_0\end{cases}$$

The field expressions can now be obtained from the potential U by [17]–[19]. Note that because the field will be TE to the z direction, this implies that $E_\xi = E_\eta = H_\phi = 0$. The continuity of E_ϕ at $\xi = \xi^*$ must now be imposed on [17], and from this condition the following is obtained:

$$A_n F_0\left(\frac{C_n}{4k}, \frac{1}{2}K\xi^{*2}\right) = B_n H_0^1\left(\frac{C_n}{4k}, \frac{1}{2}K\xi^{*2}\right)$$

and thus,

$$[59]\quad A_n = B_n \frac{H_0^1\left(\frac{C_n}{4K}, \frac{1}{2}K\xi^{*2}\right)}{F_0\left(\frac{C_n}{4K}, \frac{1}{2}K\xi^{*2}\right)}$$

Also, the appropriate boundary condition at a current source must be applied. This can be expressed in vector form as

$$[60]\quad \hat{\boldsymbol{n}} \times (\boldsymbol{H}^{\mathrm{I}} - \boldsymbol{H}^{\mathrm{II}}) = \boldsymbol{J}_s(\xi, \eta)$$

where $\hat{\boldsymbol{n}}$ is the unit normal into region I and $\boldsymbol{J}_s$ is the current sheet at the interface between region I and region II. Here, $\hat{\boldsymbol{n}} = -\hat{a}_\xi$ and $\boldsymbol{J}_s = \boldsymbol{J}$ of [57]. Thus, applying the boundary condition of [60] to the problem at hand at $\xi = \xi^*$, we get

$$[61]\quad H_\eta^{\mathrm{II}}(\xi^*, \eta) - H_\eta^{\mathrm{I}}(\xi^*, \eta) = J_\phi(\eta)\delta(\xi^* - \xi^*)\hat{a}_\phi = J_\phi(\eta)\hat{a}_\phi$$

Substituting [19] into [61], one obtains

$$[62]\quad J_\phi(\eta) = \frac{i\omega\epsilon}{\eta K\sqrt{\xi^{*2} + \eta^2}} \times \sum\left[B_n H_0^{1\prime}\left(\frac{C_n}{4K}, \frac{1}{2}K\xi^{*2}\right) - A_n F_0'\left(\frac{C_n}{4K}, \frac{1}{2}K\eta^{*2}\right)\right] \times F_0\left(\frac{C_n}{4K}, \frac{1}{2}K\eta^2\right)$$

where the prime represents differentiation with respect to the argument $z = \frac{1}{2}K\xi^2$. Applying [59] to the result of [62] and performing some algebraic manipulations, we arrive at

$$[63]\quad \frac{-i\eta K\sqrt{\xi^{*2} + \eta^2}}{\omega\epsilon}J_\phi(\eta) = \sum_n B_n\left[\frac{H_0^{1\prime}F_0 - F_0'H_0}{F_0\left(\frac{C_n}{4K}, \frac{1}{2}K\xi^{*2}\right)}\right] \times F_0\left(\frac{-C_n}{4K}, \frac{1}{2}K\eta^2\right)$$

where the argument of the wave functions in the numerator is the same as that of the denominator. Now recalling the Wronskian relation for the Coulomb wave functions

$$F_0'G_0 - F_0G_0' = 1$$

and recalling that

$$H_0^1 = G_0 + iF_0$$

TABLE 1. Eigenvalues and normalization constant for the Dirichlet case (focal length = 1 m)

	100 MHz		250 MHz		500 MHz	
n	λ_n	N	λ_n	N	λ_n	N
1	0.5083	1.4072	−0.7868	1.5105	−2.8482	1.2835
2	2.5904	1.0893	0.3574	1.6910	−1.3326	1.6026
3	5.8261	0.9063	1.6424	1.4426	−0.2952	1.8698
4	10.240	0.7925	3.3919	1.2568	0.5911	1.8304
5			5.6191	1.1289	1.6480	1.6289
6			8.3209	1.0340	2.9597	1.4781
7					4.5213	1.3657
8					6.3269	1.2770
9					8.3735	1.2043

TABLE 2. Eigenvalues and normalization constant for the Neumann case (focal length = 1 m)

	100 MHz		250 MHz		500 MHz	
n	λ_n	N	λ_n	N	λ_n	N
1	−0.2853	1.2951	−1.7051	1.1140	−4.1067	0.9635
2	1.4408	1.2257	−0.1828	1.6856	−2.0163	1.4433
3	4.1050	0.9839	0.9510	1.5658	−0.7743	1.7475
4	7.9360	0.8433	2.4663	1.3383	0.1426	1.8993
5			4.4589	1.1868	1.0895	1.7245
6			6.9264	1.0779	2.2746	1.5466
7			9.8667	0.9945	3.7134	1.4177
8					5.3987	1.3186
9					7.3261	1.2387
10					9.4931	1.1722

TABLE 3. Eigenvalues and normalization constant for the Robin case (focal length = 1 m)

	100 MHz		250 MHz		500 MHz	
n	λ_n	N	λ_n	N	λ_n	N
1	0.1161	1.4991	−1.1043	1.4409	−3.2193	1.2492
2	1.8132	1.2051	0.0852	1.7392	−1.6168	1.5560
3	4.5313	0.9782	1.2410	1.5298	−0.5186	1.8323
4	8.3900	0.8414	2.8113	1.3210	0.3580	1.8864
5			4.8424	1.1784	1.3408	1.6894
6			7.3367	1.0734	2.5666	1.5256
7			10.2960	0.9920	4.0379	1.4048
8					5.7492	1.3102
9					7.6977	1.2330
10					9.8820	1.1682

we see that

$$H_0^{1\prime}F_0 - F_0'H_0^1 = (G_0' + iF_0')F_0 - F_0'(G_0 + iF_0)$$
$$= G_0'F_0 - G_0F_0' = -1$$

Thus [63] becomes

$$[64]\quad \frac{-i\eta K\sqrt{\xi^{*2}+\eta^2}}{\omega\epsilon} J_\phi(\eta) = \sum_n \left[\frac{B_n}{F_0\left(\frac{-C_n}{4K}, \frac{1}{2}K\xi^{*2}\right)}\right] \times F_0\left(\frac{-C_n}{4K}, \frac{1}{2}K\eta^2\right)$$

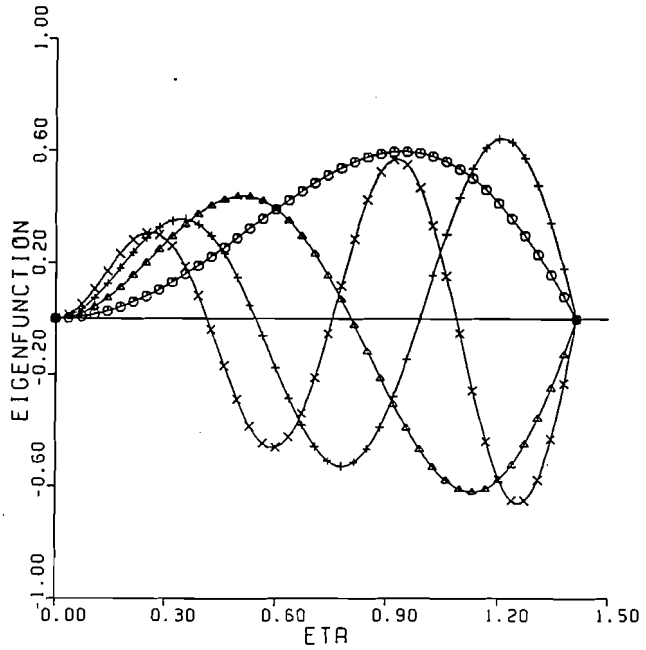

FIG. 2. Eigenfunctions for Dirichlet conditions. Frequency = 100 MHz; focal length = 1 m. ○: $\lambda_n = 0.50833$, $N = 1.40726$; △: $\lambda_n = 2.59043$, $N = 1.08930$; +: $\lambda_n = 5.82614$, $N = 0.90634$; ×: $\lambda_n = 10.23953$; $N = 0.79249$.

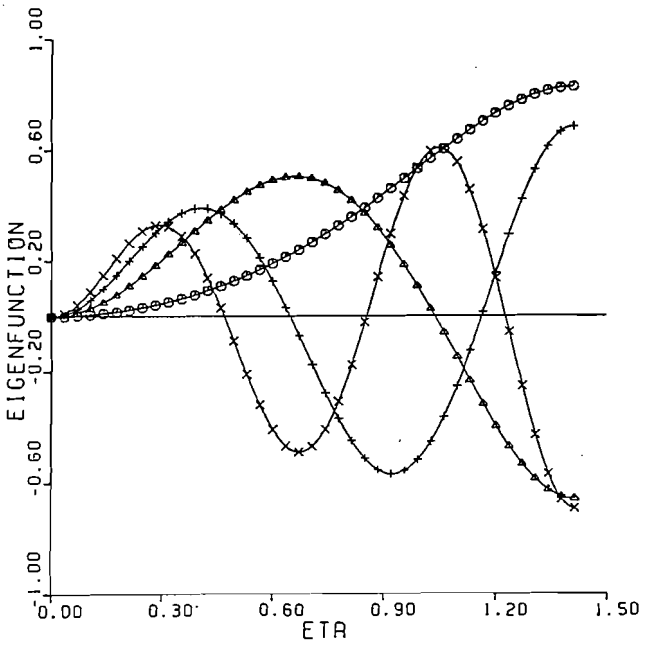

FIG. 3. Eigenfunctions for Neumann conditions. Frequency = 100 MHz; focal length = 1 m. ○: $\lambda_n = -0.28530$, $N = 1.29514$, △: $\lambda_n = 1.44084$, $N = 1.22575$; +: $\lambda_n = 4.10496$, $N = 0.98391$; ×: $\lambda_n = 7.93603$, $N = 0.84328$.

This can be recognized as the generalized Fourier transform of the function on the left with the Fourier coefficient being enclosed in the brackets. Therefore, using the orthogonality property of the regular Coulomb wave functions, which was derived previously, we can obtain the coefficients B_n. Multiplying [64] by $(2/z)F_0(-C_n/4K), z)$, where $z = \frac{1}{2}K\eta^2$, and integrating over the range $0 < z < z_0$, where $z_0 = \frac{1}{2}K\eta_0^2$, we arrive at

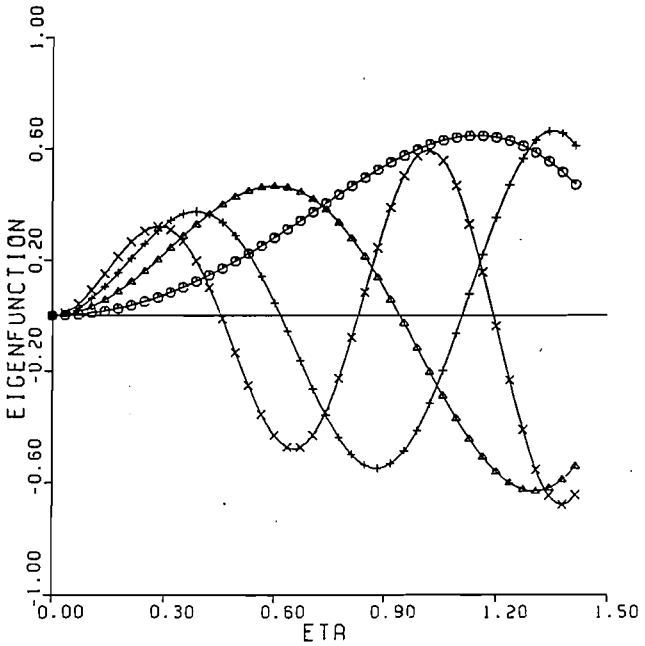

FIG. 4. Eigenfunctions for Robin conditions. Frequency = 100 MHz; focal length = 1 m. O: $\lambda_n = 0.11608$, $N = 1.49910$; △: $\lambda_n = 1.81315$, $N = 1.20509$; +: $\lambda_n = 4.53125$, $N = 0.97824$; ×: $\lambda_n = 8.39000$, $N = 0.84139$.

$$B_n = \frac{iK}{\omega\epsilon N_n^2} F_0\left(\frac{C_n}{4K}, \frac{1}{2} K\xi^{*2}\right) \int_0^{z_0} \eta\sqrt{\xi^{*2}+\eta^2} \times \left(\frac{2}{z}\right) J_\phi(\eta) F_0\left(\frac{-C_n}{4K}, z\right) dz$$

or

$$[65] \quad B_n = \frac{i4K}{\omega\epsilon N_n^2} F_0\left(\frac{C_n}{4K}, \frac{1}{2} K\xi^{*2}\right) \int_0^{\eta_0} \sqrt{\xi^{*2}+\eta^2} J_\phi(\eta) F_0 \times \left(\frac{-C_n}{4K}, \frac{1}{2} K\eta^2\right) d\eta$$

where N_n represents the normalization constant for each eigenvalue.

For a current ring, $J_\phi(\eta)$ can be expressed as

$$[66] \quad J_\phi(\eta) = J_{\text{loop}}\delta(\eta - \eta^*), \qquad \eta^* \leq \eta_0$$

where J_{loop} represents the magnitude of the current flowing in the loop. Substitution of this into [65] yields

$$[67] \quad B_n = \frac{i4KJ_{\text{loop}}\sqrt{\xi^{*2}+\eta^{*2}}}{\omega\epsilon N_n^2} F_0\left(\frac{-C_n}{4K}, \frac{1}{2} K\eta^{*2}\right) F_0 \times \left(\frac{C_n}{4K}, \frac{1}{2} K\xi^{*2}\right)$$

and from [59]

$$[68] \quad A_n = \frac{i4KJ_{\text{loop}}\sqrt{\xi^{*2}+\eta^{*2}}}{\omega\epsilon N_n^2} F_0\left(\frac{-C_n}{4K}, \frac{1}{2} K\eta^{*2}\right) H_0^1 \times \left(\frac{C_n}{4K}, \frac{1}{2} K\xi^{*2}\right)$$

As can be seen from [67] and [68], the series coefficients A_n and B_n are only functions of the eigenvalue, as the notation used (n subscript) would imply. If J_{loop} is set to

$$[69] \quad J_{\text{loop}} = \frac{\omega\epsilon}{4K\sqrt{\xi^{*2}+\eta^{*2}}}$$

then the equations for the coefficients simplify to

$$[70] \quad B_n = \frac{i}{N_n^2} F_0\left(\frac{-C_n}{4K}, \frac{1}{2} K\eta^{*2}\right) F_0\left(\frac{C_n}{4K}, \frac{1}{2} K\xi^{*2}\right)$$

and

$$[71] \quad A_n = \frac{i}{N_n^2} F_0\left(\frac{-C_n}{4K}, \frac{1}{2} K\eta^{*2}\right) H_0^1\left(\frac{C_n}{4K}, \frac{1}{2} K\xi^{*2}\right)$$

These equations have been used to calculate the first few coefficients for a paraboloid with a focal length equal to 1 m and source frequencies of 100, 250, and 500 MHz. These are the same frequencies for which the eigenvalues were calculated in the previous section. Calculations have been made for a current ring of radius 0.5 m located in the plane of the focal point. This current ring can be represented by letting $\xi^* = \frac{1}{\sqrt{2}}$ and $\eta^* = \frac{1}{\sqrt{2}}$. Note that both coordinates have the same value because the ring is located in the focal plane. The coefficients for the Dirichlet boundary condition are shown in Table 4 for all three frequencies. The Neumann and the Robin boundary-condition cases are also shown in Tables 5 and 6, respectively.

As seen in the tables, the coefficients become smaller as the mode number n increases. This is expected as similar results appear in conical and other waveguides. Thus, only the first few modes actually propagate down the waveguide with the higher order modes being highly attenuated.

6. Application to the paraboloidal reflector

Up to now, the fields inside an infinite paraboloid have been determined. The logical step now is to consider the finite paraboloid and to determine the fields exterior to it. The paraboloidal reflector is treated as an aperture antenna, and the *field-equivalence principle* or *Huygens' principle* is used to determine the far field from the antenna. The far field is represented in spherical coordinates (r, θ, ϕ) and is plotted as a function of θ. Of course, the assumption of symmetry of the fields with respect to ϕ is still made so that the field expressions of the previous sections can be used. Thus, the far-field patterns are also symmetric in ϕ.

The problem of the finite paraboloid with current-loop sources about the axis of symmetry can be transformed into an equivalent problem by considering the closed surface S shown in Fig. 5. This surface S is made up of the finite paraboloid itself plus the paraboloidal aperture surface described by $\xi = \xi_0$ for $0 < \eta < \eta_0$. The outward normal on the aperture surface is given by $\hat{n} = \hat{a}_\xi$. The fields outside the surface S are denoted by $\boldsymbol{E}_1$ and $\boldsymbol{H}_1$ while the fields inside are denoted by $\boldsymbol{E}$ and $\boldsymbol{H}$. The equivalent problem of Fig. 5 is shown in Fig. 6. The original current-loop source that was interior to the closed surface S is removed with equivalent sources $\boldsymbol{J}_s(\xi_0, \eta)$ and $\boldsymbol{M}_s(\xi_0, \eta)$ placed on the surface $\xi = \xi_0$. The current on the outside walls of the finite paraboloid is assumed to equal zero. A form of the equivalence principle, known as *Love's equivalence principle* (see ref. 6) is now used, which sets the field inside the surface S equal to zero. The equivalent sources are given by

$$[72] \quad \boldsymbol{J}_s = \hat{n} \times \boldsymbol{H}_1 = \hat{a}_\xi \times \boldsymbol{H}_1$$

and

$$[73] \quad \boldsymbol{M}_s = -\hat{n} \times \boldsymbol{E}_1 = -\hat{a}_\xi \times \boldsymbol{E}_1$$

TABLE 4. Eigenvalues and series coefficients for the Dirichlet case (focal length = 1 m)

100 MHz		250 MHz		500 MHz	
λ_n	B_n/i	λ_n	B_n/i	λ_n	B_n/i
0.5083	0.8315×10^{-1}	−0.7868	0.9134×10^{-1}	−2.8482	0.3022×10^{-1}
2.5904	0.3975×10^{-3}	0.3574	0.2402	−1.3326	−0.1819
5.8261	-0.1634×10^{-6}	1.6424	-0.2067×10^{-1}	−0.2952	-0.3992×10^{-1}
10.2400	-0.3671×10^{-12}	3.3919	-0.7448×10^{-3}	0.5911	−0.2203
		5.6191	0.3648×10^{-5}	1.6480	-0.5856×10^{-1}
		8.3209	0.3667×10^{-8}	2.9597	0.1915×10^{-1}
				4.5213	-0.1423×10^{-4}
				6.3269	-0.2087×10^{-4}
				8.3735	0.5161×10^{-7}

TABLE 5. Eigenvalues and series coefficients for the Neumann case (focal length = 1 m)

100 MHz		250 MHz		500 MHz	
λ_n	B_n/i	λ_n	B_n/i	λ_n	B_n/i
−0.2853	0.1300	−1.7051	-0.3375×10^{-1}	−4.1067	0.1927×10^{-2}
1.4408	0.1313×10^{-1}	−0.1828	0.3030	−2.0163	0.1485×10^{-1}
4.1050	-0.6222×10^{-5}	0.9510	0.3765×10^{-1}	−0.7743	−0.2924
7.9360	-0.5142×10^{-9}	2.4663	-0.7351×10^{-2}	0.1426	0.4041×10^{-1}
		4.4589	-0.1253×10^{-5}	1.0895	−0.2495
		6.9264	0.1963×10^{-6}	2.2746	0.2932×10^{-1}
		9.8667	-0.1071×10^{-10}	3.7134	0.3661×10^{-2}
				5.3987	-0.1221×10^{-3}
				7.3261	-0.1208×10^{-5}
				9.4931	0.1260×10^{-7}

TABLE 6. Eigenvalues and series coefficients for the Robin case (focal length = 1 m)

100 MHz		250 MHz		500 MHz	
λ_n	B_n/i	λ_n	B_n/i	λ_n	B_n/i
0.1161	0.1088	−1.1043	0.1087×10^{-1}	−3.2193	0.1642×10^{-1}
1.8132	0.4580×10^{-2}	0.0852	0.3032	−1.6168	-0.7445×10^{-1}
4.5313	-0.2984×10^{-5}	1.2410	-0.6194×10^{-2}	−0.5186	−0.1847
8.3900	-0.1319×10^{-9}	2.8113	-0.3394×10^{-2}	0.3580	-0.7900×10^{-1}
		4.8424	0.8564×10^{-5}	1.3408	−0.1604
		7.3367	0.6537×10^{-7}	2.5666	0.2932×10^{-1}
		10.2960	-0.1019×10^{-10}	4.0379	0.1215×10^{-2}
				5.7492	-0.6892×10^{-4}
				7.6977	-0.2510×10^{-6}
				9.8820	0.5416×10^{-8}

For $\boldsymbol{E}_1$ and $\boldsymbol{H}_1$ at the surface $\xi = \xi_0$, we use the field that would have existed if the paraboloid was infinite. This is standard procedure in the analysis of conical horns and is used here because of the close resemblance between the problems. Thus for the problem of the current loop, the field is TE to the z axis and therefore [72] and [73] become

$$[74]\quad J_s = H_\eta(\xi_0, \eta)\hat{a}_\phi = J_\phi(\xi_0, \eta)\hat{a}_\phi, \qquad 0 < \eta < \eta_0$$

and

$$[75]\quad M_s = E_\phi(\xi_0, \eta)\hat{a}_\eta = M_\eta(\xi_0, \eta)\hat{a}_\eta, \qquad 0 < \eta < \eta_0$$

The far field can now be obtained from the equivalent sources by using the standard auxiliary potentials A and F. For far-field calculations, we make the usual approximation (given by Balanis (27)). If these approximations and the equivalent surface-current expressions are used, then the far-field auxiliary potentials can be expressed as

$$[76]\quad A = \frac{\mu}{4\pi}\int_S\int J_s \frac{e^{-ikR}}{R}\,dS' \approx \frac{\mu\, e^{-ikr}}{4\pi r}\tilde{N}_A$$

where

$$[77]\quad N_A = \int_S\int J_s\, e^{-ikr\cos\psi}\,dS'$$

and

$$[78]\quad F = \frac{\epsilon}{4\pi}\int_S\int J_s \frac{e^{-ikR}}{R}\,dS' \approx \frac{\epsilon\, e^{-ikr}}{4\pi r}L_F$$

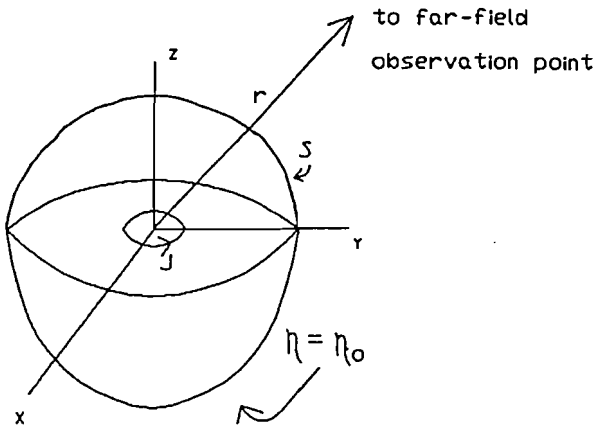

FIG. 5. Current loop inside paraboloid.

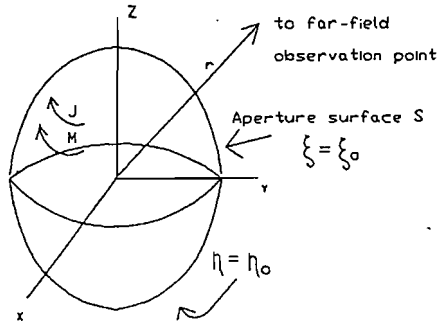

FIG. 6. Equivalent problem using equivalent current sources.

where

$$[79] \quad L_F = \int_S \int M_s e^{-ikr\cos\psi} \, dS'$$

where ψ is the angle between the vectors r and r', s is the paraboloidal surface, r is the distance from the origin to the observation point, r' is the distance from the origin to the source point, and $R = |r - r'|$. The vectors N_A and L_F are sometimes called the radiation vectors.

It should be noted at this point that the relations given by [76] and [78] are only valid for the rectangular components of the auxiliary potentials. Thus, the required equivalent sources for use in these equations and equations derived from these must be expressed in terms of the rectangular components. Because the fields we have determined previously are expressed in terms of rotation-paraboloidal components, it is useful to write the rectangular current components for the above equations in terms of rotation-paraboloidal coordinates. To accomplish this we turn to the *law of transformation of vectors* (see ref. 3). This law states that if we transform the components of a vector F from one curvilinear coordinate system (ξ_1, ξ_2, ξ_3) with scale factors (h_1, h_2, h_3) to another coordinate system (ξ_1', ξ_2', ξ_3') with scale factors (h_1', h_2', h_3'), then the components in the new system must be related to the components in the old system by the relations

$$[80] \quad F_n' = \sum_m \gamma_{nm} F_m$$

where

$$[81] \quad \gamma_{nm} = \left(\frac{h_m}{h_n'}\right)\left(\frac{\partial \xi_m}{\partial \xi_n'}\right) = \left(\frac{h_n'}{h_m}\right)\left(\frac{\partial \xi_n'}{\partial \xi_m}\right)$$

Thus the transformation from rotation-paraboloidal components to rectangular components can be written as

$$[82] \quad J_x = \frac{\eta' \cos\phi'}{\sqrt{\xi'^2 + \eta'^2}} J_\xi + \frac{\xi' \cos\phi'}{\sqrt{\xi'^2 + \eta'^2}} J_\eta - \sin\phi' J_\phi$$

$$[83] \quad J_y = \frac{\eta' \sin\phi'}{\sqrt{\xi'^2 + \eta'^2}} J_\xi + \frac{\xi' \sin\phi'}{\sqrt{\xi'^2 + \eta'^2}} J_\eta + \cos\phi' J_\phi$$

$$[84] \quad J_z = \frac{\xi'}{\sqrt{\xi'^2 + \eta'^2}} J_\xi - \frac{\eta'}{\sqrt{\xi'^2 + \eta'^2}} J_\eta$$

Similar results are also obtained for the components of the magnetic current density required in [79].

As the radiated fields are usually determined in spherical components, the rectangular unit vectors can be transformed into spherical unit vectors using the transformation from rectangular components to spherical components given by

$$\hat{a}_x = \hat{a}_r \sin\theta\cos\phi + \hat{a}_\theta \cos\theta\cos\phi - \hat{a}_\phi \sin\phi$$

$$[85] \quad \hat{a}_y = \hat{a}_r \sin\theta\sin\phi + \hat{a}_\theta \cos\theta\sin\phi + \hat{a}_\phi \cos\phi$$

$$\hat{a}_z = \hat{a}_r \cos\theta - \hat{a}_\theta \sin\theta$$

The variables in these expressions are not primed as they were in [82]–[84] because there they represented coordinates at the source points and in this transformation they represent coordinates at the observation points.

The auxiliary potentials could now be calculated by substituting [85] and [82]–[84] into [76] and [78]. Our problem is greatly simplified because not all the components of the current densities exist. Once the auxiliary potentials have been found, the fields can be obtained from the relations

$$[86] \quad E = -i\omega A - i\frac{1}{\omega\mu\epsilon}\nabla(\nabla\cdot A) - \frac{1}{\epsilon}\nabla\times F$$

and

$$[87] \quad H = \frac{1}{\mu}\nabla\times A - i\omega F - i\frac{1}{\omega\mu\epsilon}\nabla(\nabla\cdot F)$$

It can be shown (see ref. 27, p. 455) that the far field can be approximated by the set of relations

$$E_r(\theta,\phi) \approx 0$$

$$[88] \quad E_\theta(\theta,\phi) \approx \frac{-iK}{4\pi r} e^{-iKr}\left(L_{F\phi} + \sqrt{\frac{\mu}{\epsilon}} N_{A\theta}\right)$$

$$E_\phi(\theta,\phi) \approx \frac{iK}{4\pi r} e^{-iKr}\left(L_{F\theta} - \sqrt{\frac{\mu}{\epsilon}} N_{A\phi}\right)$$

and

$$H_r(\theta,\phi) \approx 0$$

$$[89] \quad H_\theta(\theta,\phi) \approx \frac{iK}{4\pi r} e^{-iKr}\left(N_{A\phi} - \sqrt{\frac{\epsilon}{\mu}} L_{F\theta}\right)$$

$$H_\phi(\theta,\phi) \approx \frac{-iK}{4\pi r} e^{-iKr}\left(N_{A\theta} + \sqrt{\frac{\epsilon}{\mu}} L_{F\phi}\right)$$

where $N_{A\phi}$, $N_{A\theta}$, $L_{F\theta}$, and $L_{F\phi}$ are obtained from [77] and [79] and are functions of θ and ϕ. Thus to obtain the far field, all that is required is that we solve [88] and [89]. After all the coordinate transformations have been applied to the electric and magnetic current densities of [74] and [75] and after extensive

simplifications, the required radiation vectors can be expressed as

$$[90]\quad N_{A\theta} = \xi_0 \cos\theta \int_0^{2\pi}\int_0^{\eta_0} \sin(\phi-\phi') J_\phi(\xi_0,\eta') \times e^{iK\Theta}\eta'\sqrt{\xi_0^2+\eta'^2}\,d\eta'\,d\phi'$$

$$[91]\quad N_{A\phi} = \xi_0 \int_0^{2\pi}\int_0^{\eta_0} \cos(\phi-\phi') J_\phi(\xi_0,\eta') \times e^{iK\Theta}\eta'\sqrt{\xi_0^2+\eta'^2}\,d\eta'\,d\phi'$$

$$[92]\quad L_{F\theta} = \xi_0 \int_0^{2\pi}\int_0^{\eta_0} [\xi_0\cos\theta\cos(\phi-\phi') + \eta'\sin\theta] \times M_\eta(\xi_0,\eta')\,e^{iK\Theta}\eta'\,d\eta'\,d\phi'$$

$$[93]\quad L_{F\phi} = \xi_0^2 \int_0^{2\pi}\int_0^{\eta_0} \sin(\phi'-\phi) M_\eta(\xi_0,\eta')\,e^{iK\Theta}\eta'\,d\eta'\,d\phi'$$

where

$$[94]\quad \Theta = \left[\xi_0\eta'\sin\theta\cos(\phi-\phi') + \frac{1}{2}(\xi_0^2-\eta'^2)\cos\theta\right]$$

The equivalent current densities can be expressed as

$$[95]\quad J_\phi(\xi_0,\eta') = H_\eta(\xi_0,\eta') = \frac{i\omega\epsilon}{\eta' K\sqrt{\xi_0^2+\eta'^2}} \sum_n B_n H_0^{1\prime}(\lambda_n, \tfrac{1}{2}K\xi_0^2) F_0 \times (-\lambda_n, \tfrac{1}{2}K\eta'^2)$$

and

$$[96]\quad M_\eta(\xi_0,\eta') = E_\phi(\xi_0,\eta') = \frac{1}{\xi_0\eta'} \sum_n B_n H_0^1(\lambda_n, \tfrac{1}{2}K\xi_0^2) F_0 \times (-\lambda_n, \tfrac{1}{2}K\eta'^2)$$

These expressions can now be substituted into [90]–[94] and we can express the radiation-vector components, for each mode n, as

$$[97]\quad N_{A\theta_n} = \frac{i\omega\epsilon}{K} B_n \xi_0 \cos\theta H_0^{1\prime}(\lambda_n, \tfrac{1}{2}K\xi_0^2) \times \int_0^{2\pi}\int_0^{\eta_0} \sin(\phi-\phi') F_0(-\lambda_n, \tfrac{1}{2}K\eta'^2)\,e^{iK\Theta}\,d\eta'\,d\phi'$$

$$[98]\quad N_{A\phi_n} = \frac{i\omega\epsilon}{K} B_n \xi_0 H_0^{1\prime}(\lambda_n, \tfrac{1}{2}K\xi_0^2) \times \int_0^{2\pi}\int_0^{\eta_0} \cos(\phi-\phi') F_0(-\lambda_n, \tfrac{1}{2}K\eta'^2)\,e^{iK\Theta}\,d\eta'\,d\phi'$$

$$[99]\quad L_{F\theta_n} = B_n H_0^1(\lambda_n, \tfrac{1}{2}K\xi_0^2) \times \int_0^{2\pi}\int_0^{\eta_0} [\xi_0\cos\theta\cos(\phi-\phi') + \eta'\sin\theta] F_0 \times (-\lambda_n, \tfrac{1}{2}K\eta'^2)\,e^{iK\Theta}\,d\eta'\,d\phi'$$

and

$$[100]\quad L_{F\phi_n} = B_n \xi_0 H_0^1(\lambda_n, \tfrac{1}{2}K\xi_0^2) \times \int_0^{2\pi}\int_0^{\eta_0} \sin(\phi'-\phi) F_0(-\lambda_n, \tfrac{1}{2}K\eta'^2)\,e^{iK\Theta}\,d\eta'\,d\phi'$$

The radiation vectors can be obtained from the above expressions by applying a summation over n. This should turn out to be necessary for the first few terms only because the series coefficients, B_n, converge rapidly. However, the problem with the determination of these radiation-vector components is in the calculation of the Coulomb wave function of the third kind, which is present in all four expressions of [97]–[100]. Calculation of these functions entails calculation of the logarithmic Coulomb wave functions, which are in general, very difficult to compute. The problem arises because of the need for values of the logarithmic function for negative parameters. That is, when the eigenvalue λ_n is negative, which is the case for the first few modes, the parameter for which the logarithmic wave function must be calculated is also negative as can be seen in the expressions. This is not a problem for the regular wave functions because we have a series representation that converges fairly well, but for the logarithmic functions, the series representation does not yield to simple computations. The alternative naturally would be to integrate the equation, with the negative parameter, using a method such as the Runge–Kutta method, but this is useless without some initial values for the function and its derivative. The function values at the turning points, which were used previously, are of no use because these are defined for a positive parameter only. The function value at $z = 0$ is defined by [A25], but its derivative, which would also be required in the Runge–Kutta technique, is undefined as can be seen from [A26]. There are no other published results that would give us starting values when the parameter is negative. This is primarily due to the fact that in the field of nuclear physics, where these functions are normally encountered, a negative parameter has no physical significance. Thus, the computation of the exact radiated field would have to be left until a useful computation technique is found for calculating the logarithmic Coulomb wave function when the parameter is negative. Results can be obtained for the 100 MHz Dirichlet and Robin cases because all the eigenvalues are positive for those cases.

For now we proceed by calculating the radiation field for only one mode in the series expansion, except for the 100 MHz Dirichlet and Robin cases as mentioned above. This allows us to set the wave function of the third kind to unity in the radiation-vector components of [97]–[100].

Once the far field has been calculated from [88] and [89], it is a simple matter to calculate the radiation intensity $U(\theta,\phi)$. The radiation intensity can be formulated from the far-zone electric and magnetic field components as

$$[101]\quad U(\theta,\phi) = \frac{1}{2}\mathrm{Re}\,[(\hat{a}_\theta E_\theta + \hat{a}_\phi E_\phi)\times(\hat{a}_\theta H_\theta + \hat{a}_\phi H_\phi)^*] = \frac{1}{2}\sqrt{\frac{\epsilon}{\mu}}(|E_\theta|^2 + |E_\phi|^2)$$

where the asterisk superscript denotes the complex conjugate of the expression in the brackets.

Substituting [88] into [101] and normalizing the result, we obtain the relative radiation intensity $F(\theta,\phi)$ as

$$[102]\quad F(\theta,\phi) = \frac{U(\theta,\phi)}{N_u} = \left|L_{F\phi} + \sqrt{\frac{\mu}{\epsilon}}N_{A\theta}\right|^2 + \left|L_{F\theta} - \sqrt{\frac{\mu}{\epsilon}}N_{A\phi}\right|^2$$

where N_u is the required normalization constant.

The integrals of [98]–[100] were performed numerically using a 20 × 20 point Gauss–Legendre quadrature algorithm.

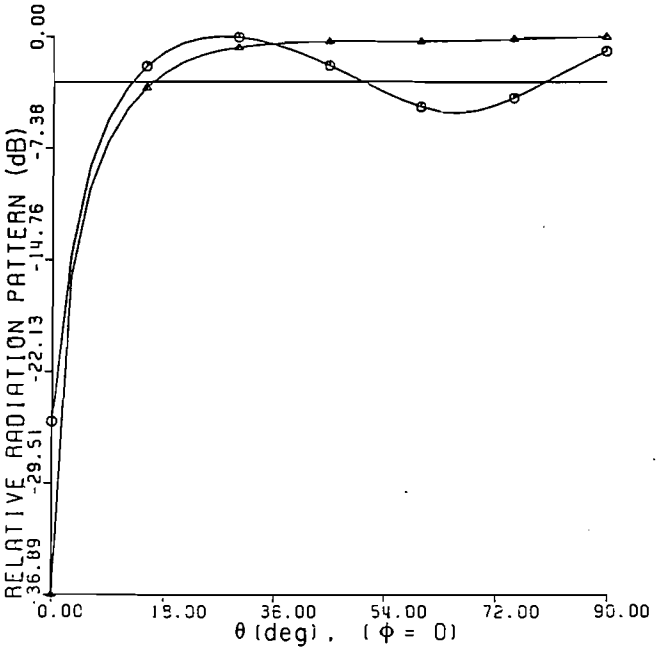

FIG. 7. Far-field radiation pattern for a numerical example. Frequency = 100 MHz; focal length = 1 m. O: Dirichlet boundary; Δ: Robin boundary.

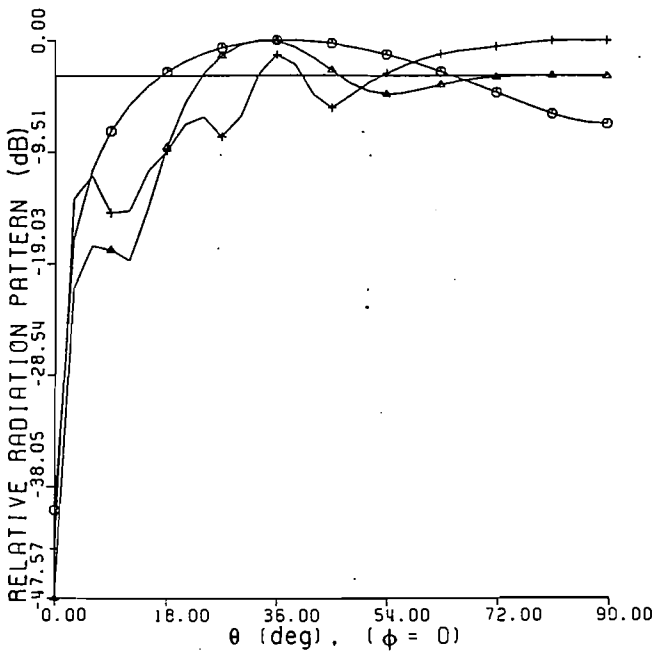

FIG. 8. Dominant mode far field for the Dirichlet condition. Focal length = 1 m. Frequencies: O, 100 MHz; Δ, 250 MHz; +, 500 MHz.

The problem that was solved was for the dominant mode of a current loop with a $\frac{1}{2}$ m radius located in the plane of the focal point of the paraboloid. Calculations were performed for all three types of boundary conditions and for all three previous frequencies of 100, 250, and 500 MHz. The exact results for the 100 MHz Dirichlet case and the 100 MHz Robin case were obtained, and the relative radiation intensities are shown in Fig. 7. The size of the paraboloid was chosen to be of 1 m in focal length, as in previous calculations. It was also assumed that the walls of the paraboloid extended up to, but not beyond, the focal plane. Thus, the aperture surface was described by the coordinate surface

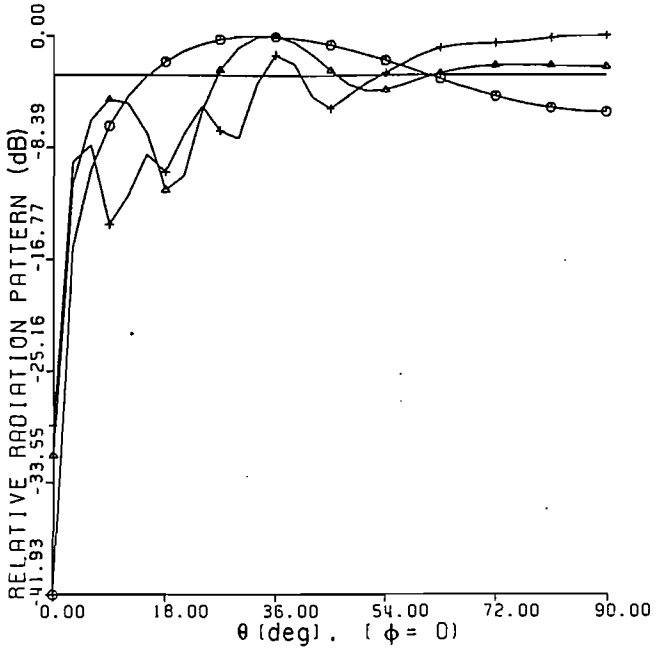

FIG. 9. Dominant mode far field for the Neumann condition. Focal length = 1 m. Frequencies: O, 100 MHz; Δ, 250 MHz; +, 500 MHz.

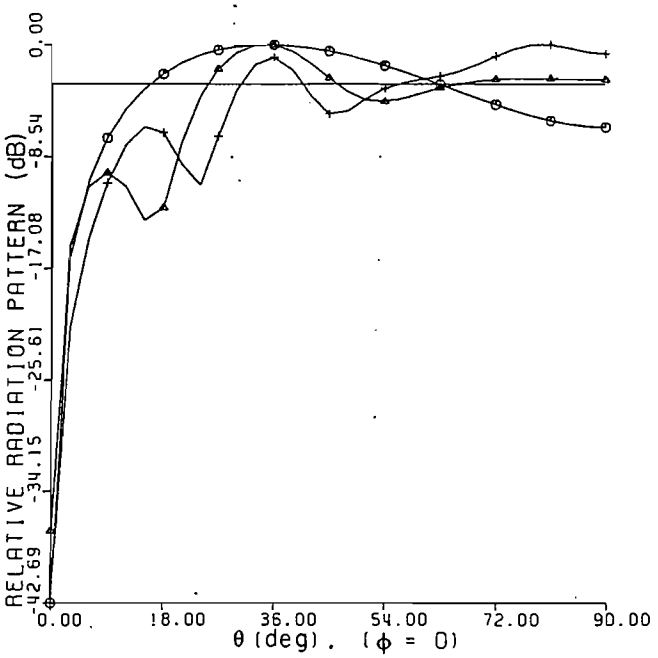

FIG. 10. Dominant mode far field for the Robin condition. Focal length = 1 m. Frequencies: O, 100 MHz; Δ, 250 MHz; +, 500 MHz.

[103] $\xi = \xi_0 = \eta_0, \qquad 0 < \eta < \eta_0$

where η_0 corresponds to a focal length of 1 m and is related to the focal length f by

[104] $\eta_0 = \sqrt{2f}$

The relative radiation intensity $F(\theta, \phi)$ was plotted as a function of θ for theta ranging from 0 to 90° at 3° intervals. Of course, because the fields were symmetric in ϕ, the relative radiation-intensity function was independent of ϕ, thus to simplify the equations, we set ϕ equal to 0°. The three plots corresponding to the three boundary conditions for the dominant mode only are shown in Figs. 8–10.

As can be seen from Fig. 7, the impedance boundary condition has an effect on the far-field radiation pattern. This is what we would expect because the field distribution inside the paraboloid is changed. Thus it seems that the Coulomb wave functions give accurate results for the far field of a current loop inside the paraboloid.

The far-field plots due to the first single mode do not seem to tell us too much about the total field. If single modes could be excited inside the paraboloid, then these plots could be useful. Efficient calculating methods are desperately required in order that the total field, such as the one plotted in Fig. 7, may be obtained for the general case and thus firmly establish the method.

7. Conclusions

A method has been presented for the evaluation of electromagnetic fields that are independent of ϕ inside a paraboloidal waveguide. The method makes use of the Coulomb wave functions as eigenfunctions for the problem. Although there is little available information on the Coulomb wave functions, their calculation has been achieved with little effort. The procedures main advantage is that it is not restricted to the high-frequency case. There are no approximations made in the analysis, and except for the assumption that the fields must be independent of ϕ, the analysis is exact. For the case of the finite paraboloid, the Kirchhoff approximation is used in the application of Huygen's principle (i.e., the incident field for the infinite paraboloid case is used as the Huygen source).

We have found that a finite impedance on the walls of the paraboloid tends to change the far-field pattern. Specifically, the far-field pattern seems to be more omnidirectional for the impedance case than for the perfectly conducting case. Whether or not this is a general result will have to wait until further calculations can be made.

Further study is required into the calculation of the irregular Coulomb wave functions for a negative parameter. Once this is done and an efficient computing technique is devised, this method of solving the paraboloidal problem should yield many interesting characteristics. Some of the more important characteristics that are required are the input impedance of the source at the focal point and the difference in radiation pattern due to sources, which may be shifted up or down along the axis away from the focal plane.

It is recommended that deep paraboloidal horns be constructed and that experimental radiation pattern results be obtained. Also, because the paraboloid is asymptotically equal to the cone, it is suggested that the possible use of the Coulomb wave functions for the conical horn problem be investigated.

Acknowledgement

The authors wish to acknowledge the financial assistance of the Natural Sciences and Engineering Research Council of Canada that made this research possible.

1. L. P. Eisenhart. Annals Math. **35**, 284 (1934).
2. J. A. Stratton. Electromagnetic theory. McGraw-Hill Book Company, Inc., New York, NY. 1941.
3. P. M. Morse and H. Feshbach. Methods of theoretical physics. Vol. 1 & 2. McGraw-Hill Book Company, Inc., New York, NY. 1953.
4. P. Moon and D. E. Spencer. Field theory handbook. Springer-Verlag, New York, NY. 1971.
5. M. Abraham. Ann. Phys. (Leipzig), **2**, 32 (1900).
6. H. Lamb. Proc. Lond. Math. Soc. **4**, 190 (1906).
7. H. Buchholtz. Z. Phys. **124**, 196 (1947).
8. C. W. Horton and F. C. Karal, Jr. J. Acoust. Soc. Am. **22**, 855 (1950).
9. C. W. Horton. J. Acoust. Soc. Am. **25**, 632 (1953).
10. E. Pinney. J. Math. Phys. (Cambridge, Mass.), **25**, 49 (1946).
11. E. Pinney. J. Math. Phys. (Cambridge, Mass.), **26**, 42 (1947).
12. H. Buchholtz. Ann. Phys. (NY), Ser. 6, **2**, 185 (1948).
13. V. A. Fock. Electromagnetic diffraction and propogation problems. Pergamon Press, London, England. 1965.
14. C. H. Wilcox. J. Math. Mech. **6**, 167 (1957).
15. C. W. Horton and F. C. Karal, Jr. J. Appl. Phys. **22**, 575 (1951).
16. A. R. Donaldson, I. P. French, and D. Midgley. Proc. Inst. Electr. Eng. Part B, **107**, 547 (1960).
17. N. S. Koshlyakov, M. M. Smirnov, and E. B. Glimer. Differential equations of mathematical physics. North-Holland Publishing Company, Amsterdam, The Netherlands. 1964.
18. A. Mohsen and M. A. K. Hamid. J. Appl. Phys. **41**, 433 (1970).
19. T. B. A. Senior. Appl. Sci. Res. Sect. B, **8**, 418 (1960).
20. T. B. A. Senior. Appl. Sci. Res. Sect. B, **8**, 437 (1960).
21. V. H. Weston. IEEE Trans. Antennas Propag. **AP-11**, 578 (1963).
22. J. LoVetri. M.Sc. Thesis. University of Manitoba, Winnipeg, Man. 1986.
23. M. Abramowitz and I. A. Stegun. Handbook of mathematical functions. Dover Publications Inc., New York, NY. 1972.
24. A. G. Mackie. Boundary value problems. Oliver and Boyd, Ltd., London, England. 1965.
25. D. W. Trim. Partial differential equations. Course Notes, University of Manitoba, Winnipeg, Man. To be published.
26. A. E. H. Love. Philos. Trans. R. Soc. London, A, **197**, 1 (1901).
27. C. A. Balanis. Antenna theory analysis and design. Harper & Row, Publishers, New York, NY. 1982.
28. National Bureau of Standards. Applied Mathematics Series 17. Tables of Coulomb wave functions. Vol. 1. U.S. Government Printing Office, Washington, DC. 1952.
29. C. Fröberg. Rev. Mod. Phys. **27**, 399 (1955).
30. A. V. Luk'Yanov, I. V. Teplov, and M. K. Akimova. Tables of Coulomb wave functions (Whittaker functions). The MacMillan Company, New York, NY. 1965.

Appendix A

In this appendix, some mathematical properties of the Coulomb wave equation and its solution, the Coulomb wave functions, will be investigated. These functions will be investigated in the form of a Sturm–Liouville system, as the ultimate goal for their use is as eigenfunctions.

The notation used here for a regular Sturm–Liouville system follows that of Trim (25), and is given by

$$[A1] \quad [r(z)y'(\lambda, z)]' + [\lambda p(z) - q(z)]y(\lambda, z) = 0, \qquad a < z < b$$

$$[A2] \quad -l_1 y'(\lambda, a) + h_1 y(\lambda, a) = 0$$

$$[A3] \quad l_2 y'(\lambda, b) + h_2 y(\lambda, b) = 0$$

The constants h_1, h_2, l_1, and l_2 in the Robin boundary conditions are real and independent of the parameter λ. The functions $p(z)$, $q(z)$, $r(z)$, and $r'(z)$ are real and continuous over the specified interval. Also, it is assumed that $p(z) > 0$ and $r(z) > 0$ for $a < z < b$. The parameter λ takes on a denumerable set of values of $\lambda_n (n = 1, 2, \ldots)$ for which the corresponding nontrivial solution of [A1] is denoted by $y_n(z) = y(\lambda_n, z)$. The $y_n(z)$'s are called the eigenfunctions of the Sturm–Liouville system and the λ_n's are the eigenvalues.

For the case of the Coulomb wave functions and the rotation-paraboloidal coordinates, the specific values of the functions in the system of [A1] are provided from [39] where

$r(z) = 1.0$, $p(z) = 2/z$, and $q(z) = -1.0$, where the range of the variable z is $0 < z < z_0$. It is noted that r, p, and q satisfy all of the necessary requirements quoted above. For the case of the paraboloidal waveguide, there is no boundary condition at $z = 0$, but only at $z = z_0$ (i.e., at the walls of the paraboloidal waveguide). Thus, the singular Sturm–Liouville system

$$[A4] \quad y_n''(z) + \left[1 + \lambda_n\left(\frac{2}{z}\right)\right] y_n(z) = 0, \qquad 0 < z < z_0$$

$$[A5] \quad l_2 y_n'(z_0) + h_2 y_n(z_0) = 0$$

arises, where at least one of l_2 and h_2 is not equal to zero. If $l_2 = 0$, we have a Dirichlet condition at $z = z_0$. If $h_2 = 0$, we have a Neumann condition at $z = z_0$. If both l_2 and h_2 exist then we have a Robin condition at $z = z_0$, which will be necessary for the impedance boundary-condition case. Thus, it is necessary to obtain numerical results for all three cases.

The above system of equations [A4]–[A5] is a singular Sturm–Liouville system because only one boundary condition exists. Thus, the general properties of a regular Sturm–Liouville system cannot be used without proof. One of the most useful of these properties that will be required in later discussion is the orthogonality of the eigenfunctions with respect to the weighting function $p(z)$.

Consider the eigenvalue–eigenfunction pairs (y_m, λ_m) and (y_n, λ_n). The differential equation satisfied by each of these eigenvalue–eigenfunction pairs is given by [A4]:

$$[A6] \quad y_n''(z) + \left[1 + \lambda_n\left(\frac{2}{z}\right)\right] y_n(z) = 0, \qquad 0 < z < z_0$$

$$[A7] \quad y_m''(z) + \left[1 + \lambda_m\left(\frac{2}{z}\right)\right] y_m(z) = 0, \qquad 0 < z < z_0$$

The following manipulations are now performed:

$$y_m\left\{y_n''(z) + \left[1 + \lambda_n\left(\frac{2}{z}\right)\right] y_n(z)\right\} - y_n\left\{y_m''(z) + \left[1 + \lambda_m\left(\frac{2}{z}\right)\right] y_m(z)\right\} = 0$$

$$y_m y_n'' - y_n y_m'' = y_n y_m(\lambda_m - \lambda_n)\frac{2}{z} = (y_m y_n')' - (y_n y_m')'$$

Integrating with respect to z over the interval, we get

$$(\lambda_m - \lambda_n)\int_0^{z_0} y_m y_n\left(\frac{2}{z}\right) dz = \begin{vmatrix} y_m(z_0) & y_m'(z_0) \\ y_n(z_0) & y_n'(z_0) \end{vmatrix} - \begin{vmatrix} y_m(0) & y_m'(0) \\ y_n(0) & y_n'(0) \end{vmatrix}$$

Now for orthogonality of the eigenfunctions with respect to the weighting function $p(z)$, the right side of the above equation must be equal to zero. The first determinant is equal to zero because of the existence of the boundary condition at $z = z_0$. That is, if one thinks of the boundary equations at $z = z_0$ for y_m and y_n as simultaneous equations in l_2 and h_2, then because these equations have nontrivial solutions (i.e., at least one of l_2 and h_2 must exist), the determinant must go to zero. The second determinant does not collapse to zero as easily as the first because there is no boundary condition at $z = 0$. We find that if we examine the properties of the solutions of the Coulomb wave equation, we see that one of the solutions is identically zero at $z = 0$. Thus this solution is orthogonal. As will be seen in later discussions, the second solution is not appropriate and thus is not used in the eigenfunction solution because it produces a singularity in the field at $z = 0$. Therefore the orthogonality of the second solution is not required.

Now that we have established orthogonality it is convenient to normalize the eigenfunctions. Thus a normalization constant, N, can be defined by

$$[A8] \quad N^2 = \int_0^{z_0} y_m y_n\left(\frac{2}{z}\right) dz$$

The eigenfunctions are divided by N to make them orthonormal.

A.1. Properties of the Coulomb wave functions

In this section the properties of the Coulomb wave functions are investigated. These properties are results obtained from many authors over a number of years (see refs. 28–30). The notation used here is that of Abramowitz and Stegun (23), which was a compilation of the properties known about the functions up to 1965. The results that will be shown here are modified to the case where $L = 0$ so that they can be directly applied to the problem at hand.

The solution of the Coulomb wave equation (see [39]) consists of the two solutions given in [41]. In the following discussions, the parameter β is used, where β is related to λ by [40]. The solution $F_0(\beta, z)$ is called the regular Coulomb wave function, while $G_0(\beta, z)$ is called the irregular or logarithmic Coulomb wave function.

A.2. The regular wave function

The regular Coulomb wave function can be expressed in terms of the confluent hypergeometric equation, i.e.,

$$F_0(\beta, z) = C_0(\beta) z e^{-iz} M(1 - i\beta, 2, 2iz)$$

where

$$[A9] \quad C_0(\beta) = \left[\frac{2\pi\beta}{(e^{\pi\beta} - 1)}\right]^{1/2}$$

A more appropriate form for numerical computations is

$$[A10] \quad F_\theta(\beta, z) = C_0(\beta) z \Phi_0(\beta, z)$$

where

$$[A11] \quad \Phi_0(\beta, z) = \sum_{n=1}^{\infty} A_n(\beta) z^{n-1}$$

and

$$[A12] \quad A_1 = 1, \quad A_2 = \beta, \quad n(n-1)A_n = 2\beta A_{n-1} - A_{n-2} \quad n > 2$$

The derivative with respect to z of the regular wave function can be computed using the relation

$$[A13] \quad F_0' = \frac{d}{dz} F_0 = C_0(\beta)\Phi_0^*(\beta, z)$$

where

$$[A14] \quad \Phi_0^* = \sum_{n=1}^{\infty} n A_n(\beta) z^{n-1}$$

The above series relations were used to compute the regular wave function for $0 < z < 5$, and for the parameter β ranging from $+5$ to -10. The results were checked with published results such as those of the National Bureau of Standards (28) and Luk'Yanov *et al.* (30). The only source found for negative

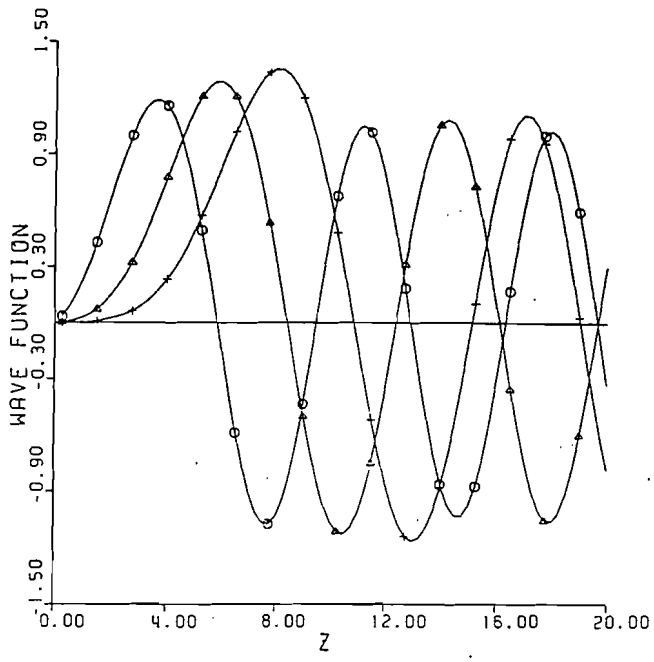

FIG. A1. Regular Coulomb wave function, $F(n, z)$. Parameters: ○, $n = 1$; △, $n = 2$; +, $n = 3$.

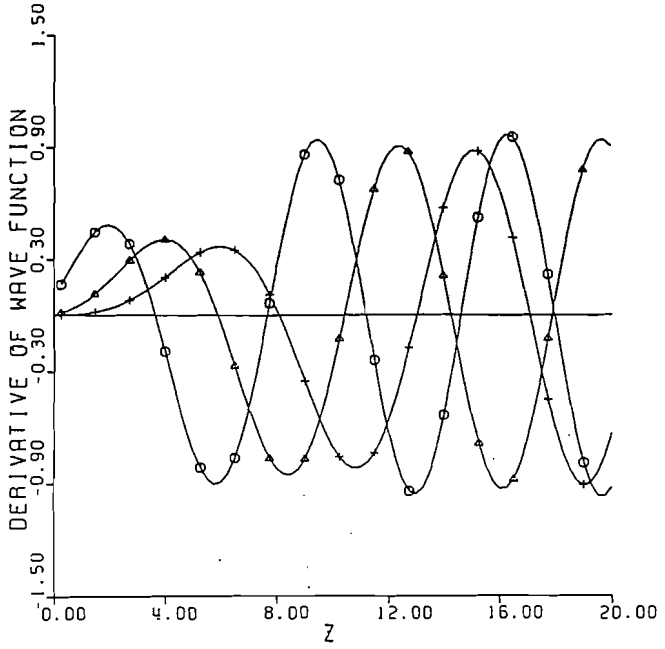

FIG. A2. Derivative of regular Coulomb wave function, $F(n, z)$. Parameters: ○, $n = 1$; △, $n = 2$; +, $n = 3$.

values of β was the national Bureau of Standards (28). The reason for the scarcity of results in this region is probably that negative values of β have no physical significance in the use of these functions to express the Coulomb field about a nucleus.

Unfortunately, the series representations given above cannot be used for all values of z and β. For different regions in the z–β plane, different methods of computation must be used (see ref. 29). One important region in this plane is called the transition region or the turning points where $z = 2\beta$. Asymptotic expansions for $z = 2\beta > 0$ are given by

$$[A15]\quad F_0(2\beta) = 0.7063326373\beta^{1/6} \times \left[1 - \frac{0.04959570165}{\beta^{4/3}} - \frac{0.00888888889}{\beta^2} - \frac{0.002455199181}{\beta^{10/3}} - \ldots\right]$$

and

$$[A16]\quad F_0'(2\beta) = 0.4086957323\beta^{-1/6} \times \left[1 + \frac{0.1728260369}{\beta^{2/3}} + \frac{0.0003174603174}{\beta^2} + \frac{0.003581214850}{\beta^{8/3}} + \ldots\right]$$

For values of z where the series solution was inaccurate, the values of the function and its derivative at the turning points were used as initial values and the differential equation was integrated using the Runge–Kutta–Verner fifth- and sixth-order method. The algorithm that was used was from the International Mathematical and Statistical Library, 1982. Calculations were performed for values of z down from the turning points and up from the turning points with a relative accuracy of 10^{-5}. Plots of the regular Coulomb wave function and its derivative are shown in Figs. A1 and A2 respectively.

As can be seen from the graphs, at the point $z = 0$ the regular Coulomb wave function takes on the value

$$[A17]\quad F_0(\beta, 0) = 0$$

while, not so obviously, its derivative takes on the vaue

$$[A18]\quad F_0'(\beta, 0) = C_0(\beta)$$

A.3. The irregular wave function

The irregular or logarithmic Coulomb wave function can be expressed in terms of the regular wave function as

$$[A19]\quad G_0(\beta, z) = \frac{2\beta}{C_0^2(\beta)} F_0(\beta, z)\left[\ln(2z) + \frac{q_0(\beta)}{p_0(\beta)}\right] + \Theta_0(\beta, z)$$

where

$$[A20]\quad \Theta_0(\beta, z) = \frac{\psi_0(\beta, z)}{C_0(\beta)}$$

and

$$\psi_0(\beta, z) = \sum_{n=1}^{\infty} a_n(\beta) z^n$$

$$[A21]\quad a_0 = 1, \qquad a_1 = 0, \qquad n(n-1)a_n = 2\beta a_{n-1} - a_{n-2} - (2n-1)2\beta A_n$$

where A_n is the same coefficient as that used in the series expansion of the regular wave function given in [A12] and $C_0(\beta)$ is given by [A9]. Also we have

$$[A22]\quad \frac{q_0(\beta)}{p_0(\beta)} = -1 + \mathrm{Re}\left[\frac{\Gamma'(1+i\beta)}{\Gamma(1+i\beta)}\right] + 2\gamma = -1 + \gamma + \beta^2 \sum_{n=1}^{\infty} \frac{1}{n(n^2+\beta^2)}$$

where γ is Euler's number, $\gamma = 0.577215665$.

Unlike the series representation for the regular Coulomb wave function, the above representation is very difficult to use in computations. Thus, the differential equation has been integrated using the same Runge–Kutta method as for the

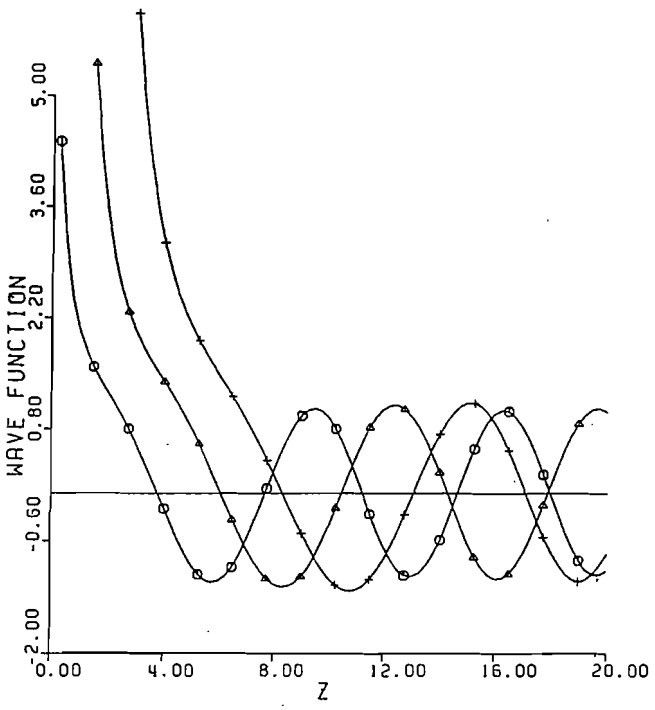

FIG. A3. Irregular Coulomb wave function, $G(n, z)$. Parameters: ○, $n = 1$; △, $n = 2$; +, $n = 3$.

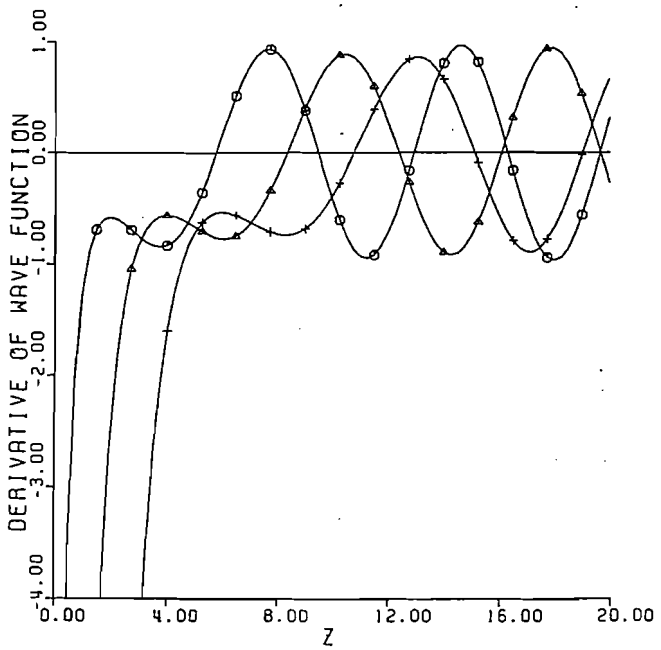

FIG. A4. Derivative of irregular Coulomb wave function, $G(n, z)$. Parameters: ○, $n = 1$; △, $n = 2$; +, $n = 3$.

regular wave function. The initial values used are also the values of the function and its derivative at the turning points, which are given by

$$[A23] \quad G_0(2\beta) = 1.223404016\beta^{1/6} \times \left[1 + \frac{0.04959570165}{\beta^{4/3}} - \frac{0.00888888889}{\beta^2} + \frac{0.002455199181}{\beta^{10/3}} - \ldots\right]$$

and

$$[A24] \quad G_0'(2\beta) = -0.7078817734\beta^{-1/6} \times \left[1 - \frac{0.1728260369}{\beta^{2/3}} + \frac{0.0003174603174}{\beta^2} - \frac{0.003581214850}{\beta^{8/3}} + \ldots\right]$$

The irregular wave functions have been calculated for the same ranges as for the regular wave functions, and the plots are shown in Figs. A3 and A4.

At the point $z = 0$, the irregular wave function can be determined from

$$[A25] \quad G_0(\beta, 0) = \frac{1}{C_0(\beta)}$$

and its derivative from

$$[A26] \quad G_0'(\beta, 0) = -\infty$$

A.4. Wave functions of the third kind

The two solutions $F_0(\beta, z)$ and $G_0(\beta, z)$ can be combined to form two alternate solutions, which we shall call Coulomb wave functions of the third kind. These new functions are defined as

$$[A27] \quad H_0^1(\beta, z) = G_0(\beta, z) + iF_0(\beta, z)$$

and

$$[A28] \quad H_0^2(\beta, z) = G_0(\beta, z) - iF_0(\beta, z)$$

These functions are useful in terms of their asymptotic representations for large z, for as z gets large,

$$[A29] \quad H_0^1(\beta, z) \rightarrow e^{i\theta_0}$$

and

$$[A30] \quad H_0^2(\beta, z) \rightarrow e^{-i\theta_0}$$

where

$$[A31] \quad \theta_\theta = z - \beta \ln(2z) + \arg[\Gamma(1 + i\beta)]$$

These functions and the method of defining them are analogous to the exponential expansions of the Hankel functions, which are defined in a similar way but should not be confused with the above functions.